

## Terbium and barium codoped mesoporous silica nanoparticles with enhanced optical properties

Kamila Zhumanova<sup>a,1</sup>, Nursalim Akhmetzhanov<sup>a,1</sup>, Moon Sung Kang<sup>b</sup>, Anara Molkenova<sup>a,c</sup>,  
Iruthayapandi Selestin Raja<sup>d</sup>, Ki Su Kim<sup>c,e,\*</sup>, Dong-Wook Han<sup>b,d,\*</sup>, Timur Sh. Atabaev<sup>a,\*</sup>

<sup>a</sup> Department of Chemistry, Nazarbayev University, Nur-Sultan 010000, Kazakhstan

<sup>b</sup> Department of Cogno-Mechatronics Engineering, Pusan National University, Busan 46241, South Korea

<sup>c</sup> Institute of Advanced Organic Materials, Pusan National University, Busan 46241, South Korea

<sup>d</sup> BIO-IT Fusion Technology Research Institute, Pusan National University, Busan 46241, South Korea

<sup>e</sup> School of Chemical Engineering, Pusan National University, Busan 46241, South Korea

### ARTICLE INFO

#### Keywords:

Nanoparticles  
Porous materials  
Optical materials and properties  
Luminescence

### ABSTRACT

In this study, we showed for the first time that barium (Ba) codoping improves the luminescent properties of terbium (Tb)-doped SiO<sub>2</sub> nanoparticles (NPs). In particular, the quantum yield (QY) of SiO<sub>2</sub>-Ba,Tb NPs was found to be ~10.7%, whereas the QY of bare SiO<sub>2</sub>-Tb NPs was only ~4.3%. Several mechanisms for luminescence enhancement have been proposed. We strongly believe that this methodology can be used to create alternative silica-based NPs with improved optical characteristics.

### 1. Introduction

Lanthanide-based nanostructures (nanophosphors) have received a lot of attention as optically stable nanoprobes for bioimaging, sensing, security, and photovoltaic applications. Fabrication simplicity, high quantum yields, nonbleaching, large Stokes shifts, and chemical stability make them more popular than traditional fluorescent organic dyes and semiconductor quantum dots [1–3]. Although these lanthanide-based nanostructures demonstrated promising results, their widespread applicability for a variety of applications is still hampered by a number of factors. First, the use of efficient but scarce and costly lanthanide elements (yttrium, gadolinium, etc.) as host materials is not practical from an economic point of view. Second, a transparent SiO<sub>2</sub> coating is usually required for surface passivation purposes. Hence, the development of low-cost optical nanoprobes with excellent optical properties is still a crucial task.

To date, several research groups have attempted to use SiO<sub>2</sub> as a host material because of their well-established synthesis protocols, chemical stability, lowcost, and nontoxicity. For example, several strategies, such as water-in-oil [4,5], thermolysis [6], and adsorption [7–9] have been proposed for lanthanide-doped SiO<sub>2</sub> NPs. Among them, water-in-oil and thermolysis methods are less preferable because of poor control over

morphology, inhomogeneous dopant distribution, synthesis complexity, and generation of chemical wastes. In the adsorption method, one can prepare the desired morphology and size of mesoporous SiO<sub>2</sub> nanostructures and later incorporate lanthanide cations into negatively charged silica pores. The main drawback of this method is that only a small amount of cations remain in SiO<sub>2</sub> NPs, which in turn results in luminescent materials with low quantum yields (QYs).

The codoping strategy can be considered one of the promising methods to resolve the issue of the low QY of metal-doped SiO<sub>2</sub> NPs prepared by adsorption methods. For example, various chemical elements, such as Zn [10], Bi [11], Li [12], Al [13], and Ba [14], are often reported as codopants to improve the optical properties of phosphor materials. In some cases, these elements can distort the local bonding around the activator, leading to a change in luminescence intensity. Hence, in the present study, we opted to employ adsorption-based codoping strategy to improve the optical properties of metal-doped SiO<sub>2</sub> NPs. Terbium was used as an optical activator, while barium was used as an earth-abundant codopant. According to a literature survey, metal codoped mesoporous SiO<sub>2</sub> NPs, especially Ba and Tb codoped SiO<sub>2</sub> have not yet been explored.

\* Corresponding authors at: Nazarbayev University (T.Sh. Atabaev) and Pusan National University (K.S. Kim & D.-W. Han).

E-mail addresses: [kisukim@pusan.ac.kr](mailto:kisukim@pusan.ac.kr) (K.S. Kim), [nanohan@pusan.ac.kr](mailto:nanohan@pusan.ac.kr) (D.-W. Han), [timur.atabaev@nu.edu.kz](mailto:timur.atabaev@nu.edu.kz) (T.Sh. Atabaev).

<sup>1</sup> Equal contribution.

## 2. Materials and methods

Mesoporous silica NPs were prepared according to recently reported protocol [9]. In brief, 10 mg of silica and X mg of  $\text{TbCl}_3 \cdot 6\text{H}_2\text{O}$  ( $X = 1, 2,$  or  $3$  mg) were dissolved in 6 mL of deionized (DI) water followed by sonication for 3 min to obtain a colloidal solution. The as-prepared colloidal solution was stirred for 24 h (700 rpm) to achieve adsorption-desorption equilibrium. Metal-activated  $\text{SiO}_2$  NPs were collected, dried, and calcinated at  $600^\circ\text{C}$  for 1 h (ramping rate of  $5^\circ\text{C}/\text{min}$ ). To prepare Tb(III) and Ba(II) codoped silica NPs, 2 mg of  $\text{TbCl}_3 \cdot 6\text{H}_2\text{O}$  and 30 mg of  $\text{Ba}(\text{NO}_3)_2$  were dissolved in 6 mL of DI water followed by the addition of 10 mg of  $\text{SiO}_2$  NPs. Further procedures were the same as described above for bare  $\text{SiO}_2$ -Tb NPs. Characterization details can be found in Supporting Information.

## 3. Results and discussion

First,  $\text{SiO}_2$ -Tb NPs with various  $\text{TbCl}_3 \cdot 6\text{H}_2\text{O}$  salt concentrations (1–3 mg) were prepared to reveal the difference in activator adsorption. Figure S1 (Supporting Information) shows that all samples yielded an average concentration of  $\sim 3.1 \pm 0.5$  wt%, demonstrating a negligible difference in Tb adsorption. Consequently, 2 mg of  $\text{TbCl}_3 \cdot 6\text{H}_2\text{O}$  was selected as the optimal loading concentration. Next, codoped  $\text{SiO}_2$  NPs were prepared by introducing Ba(II) ions. Figures S2 and S3 (Supporting Information) show EDX elemental analysis for both  $\text{SiO}_2$ -Tb and  $\text{SiO}_2$ -Ba,Tb NPs. In both cases, main elements such as Si, O, and Tb were easily detected, suggesting the successful incorporation and even distribution of Tb(III) ions. In addition, the uniform incorporation of Ba was also confirmed by EDX elemental analysis for  $\text{SiO}_2$ -Ba,Tb NPs.

We observed no significant morphological and structural difference between  $\text{SiO}_2$ -Ba,Tb NPs and  $\text{SiO}_2$ -Tb NPs; thus, morphological and structural analysis data were presented for  $\text{SiO}_2$ -Ba,Tb NPs only. Fig. 1 shows that  $\text{SiO}_2$ -Ba,Tb NPs had a well-defined quasi-spherical shape with a mean size distribution in the range of  $\sim 70$ – $80$  nm. High-resolution TEM image (Fig. 1 inset) reveals that the synthesized NPs have a well-resolved porous structure even after high-temperature calcination. According to TEM analysis, no aggregates were formed inside the  $\text{SiO}_2$  pores, indicating the uniform fixation of dopants to the pore walls. Elemental analysis revealed that Tb concentrations in both samples were nearly identical ( $\sim 3.1 \pm 0.3$  wt%), while Ba(II) content in  $\text{SiO}_2$ -Ba,Tb NPs was found to be  $\sim 1.8$  wt%.

The surface area and pore size distribution of  $\text{SiO}_2$ -Ba,Tb NPs were further studied using a nitrogen porosimeter. Fig. 2 shows the

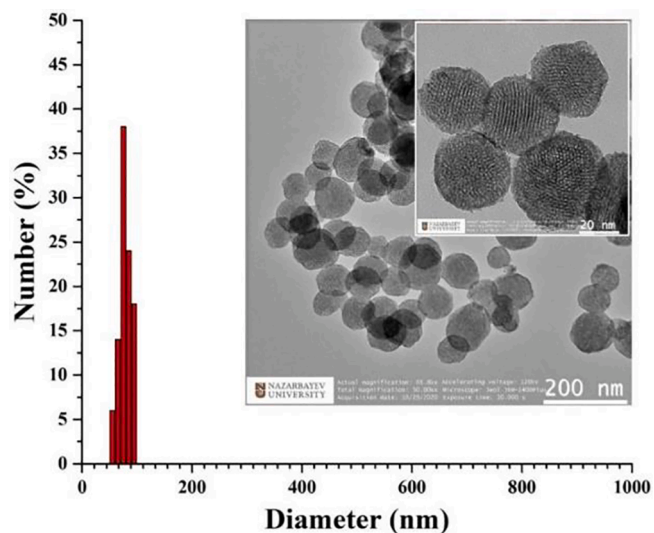


Fig. 1. Size distribution of  $\text{SiO}_2$ -Ba,Tb NPs. The inset shows low- and high-resolution TEM images of  $\text{SiO}_2$ -Ba,Tb NPs.

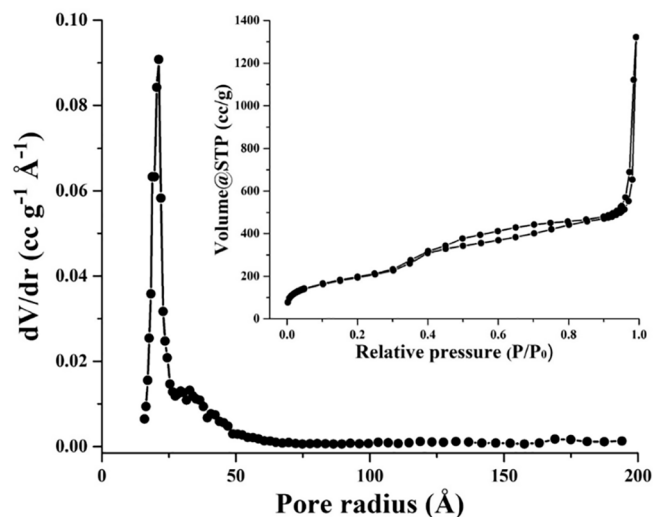


Fig. 2. BJH pore size distribution and BET nitrogen adsorption isotherms (inset) of  $\text{SiO}_2$ -Ba,Tb NPs.

Barrett–Joyner–Halenda (BJH) pore size distribution and Brunauer–Emmett–Teller (BET) surface area isotherms (inset).  $\text{SiO}_2$ -Ba,Tb NPs demonstrated a type IV adsorption-desorption isotherm with a calculated specific surface area of  $\sim 573.9$   $\text{m}^2/\text{g}$  and pore size of  $\sim 3$ – $4$  nm. For comparison, the specific surface area for undoped  $\text{SiO}_2$  NPs was  $\sim 717.3$   $\text{m}^2/\text{g}$  (data not shown). The observation of the type IV isotherm suggests the formation of a mesoporous structure with a narrow pore size distribution [15]. A decrease in surface area can be attributed to the codopants incorporation into silica pores.

The formation of silica-based NPs was further confirmed by FT-IR spectroscopy. Fig. 3 represents the corresponding FT-IR transmittance spectra showing some well-defined bands. For example, the major band at  $1068$   $\text{cm}^{-1}$  with a shoulder at approximately  $1220$   $\text{cm}^{-1}$  belongs to the asymmetric stretching vibrations of siloxane groups (Si-O-Si) [9]. The peak at  $807$   $\text{cm}^{-1}$  can be ascribed to the symmetric stretching vibrations of Si-O-Si [9]. It should be noted that no other bands were detected, suggesting the formation of pure silica structures after the thermal treatment process. The structural properties of the prepared  $\text{SiO}_2$ -Ba,Tb NPs were also assessed by XRD. The typical XRD pattern revealed a broad peak which corresponds to the amorphous structure of  $\text{SiO}_2$  (Fig. 3, inset).

The optical properties of  $\text{SiO}_2$ -Ba,Tb and  $\text{SiO}_2$ -Tb NPs were further

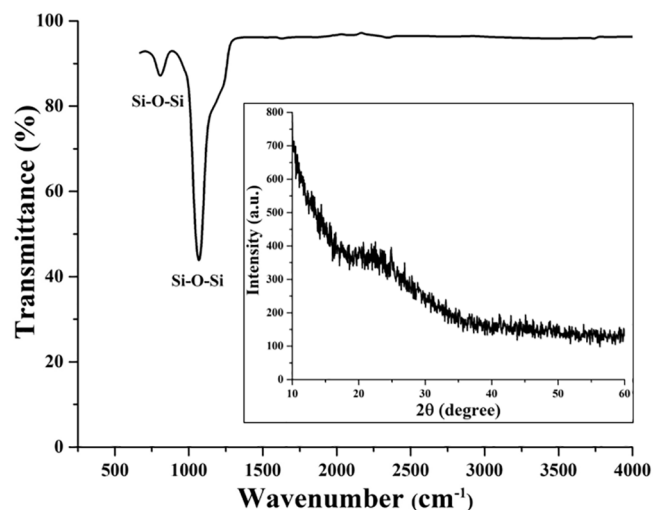


Fig. 3. FTIR analysis and XRD pattern (inset) of  $\text{SiO}_2$ -Ba,Tb NPs.

analyzed using photoluminescence (PL) spectroscopy. The QYs of these NPs were analyzed at different wavelengths in the range of 250–350 nm with a step of 5 nm. The QY scan revealed that the maximum QY values were 10.7% and 4.3% ( $\lambda_{\text{exc}} = 260$  nm) for SiO<sub>2</sub>-Ba,Tb NPs and SiO<sub>2</sub>-Tb NPs, respectively. Hence, the optimal excitation wavelength was selected to be  $\sim 260$  nm. Fig. 4 shows the room-temperature PL emission spectra of SiO<sub>2</sub>-Tb and SiO<sub>2</sub>-Ba,Tb NPs. PL analysis revealed four characteristic Tb emission peaks centered at 487 nm (<sup>5</sup>D<sub>4</sub>-<sup>7</sup>F<sub>6</sub>), 545 nm (<sup>5</sup>D<sub>4</sub>-<sup>7</sup>F<sub>5</sub>), 585 nm (<sup>5</sup>D<sub>4</sub>-<sup>7</sup>F<sub>4</sub>), and 624 nm (<sup>5</sup>D<sub>4</sub>-<sup>7</sup>F<sub>3</sub>) [16,17]. One can observe that the intensity of the <sup>5</sup>D<sub>4</sub>-<sup>7</sup>F<sub>5</sub> transition at 545 nm prevails; hence, the green color is mostly perceived to the naked eye (Fig. 4, inset). We can speculate that the enhancement of QY in SiO<sub>2</sub>-Ba,Tb NPs can be associated with the incorporation of Ba(II) ions. Among the possible options is that crystalline BaO with Tb (III) ions can be formed after the thermal treatment, which results in luminescence improvement similar to that of Al- and Tb-codoped SiO<sub>2</sub> glass [18]. Another mechanism involves better Tb(III) ion-ion separation by Ba(II) codopant, which inhibit the cross-relaxation processes [19,20]. Moreover, the luminescence enhancement can be also associated with charge transfer from Ba element, leading to the improved QY, as it shown with Ba-doped carbon dots [21]. The exact enhancement mechanism has yet to be determined and will require more sophisticated experiments in the near future. Nevertheless, a straightforward codoping strategy led to a significant luminescence enhancement of metal-doped silica NPs, which can be useful in the development of efficient silica-based optical materials.

#### 4. Conclusion

In summary, mesoporous silica NPs codoped with Tb(III) and Ba(II) ions have been successfully synthesized using a facile adsorption method. We showed that Ba(II) codoping strategy significantly improves the quantum yield of SiO<sub>2</sub>-Tb NPs by a factor of  $\sim 2.49$ . We believe that proposed method can be expanded for the fabrication of other lanthanide-doped SiO<sub>2</sub> NPs with enhanced optical properties.

#### Funding

This research was funded by Nazarbayev University FDCRDG grant (No. 240919FD3929). This work supported by the National Research Foundation of Korea (NRF) grant funded by the Korean government (MSIT) (No. 2021R1A2C2006013 and 2021M3H4A4079509). This study was financially supported by the 2022 Post-Doc. Development Program of Pusan National University.

#### CRedit authorship contribution statement

**Kamila Zhumanova:** Investigation, Formal analysis, Validation, Writing – original draft. **Nursalim Akhmetzhanov:** Investigation, Formal analysis, Validation. **Moon Sung Kang:** Formal analysis, Validation. **Anara Molkenova:** Formal analysis, Validation, Supervision. **Iruthayapandi Selestin Raja:** Formal analysis, Validation. **Ki Su Kim:** Conceptualization, Methodology, Validation, Supervision. **Dong-Wook Han:** Conceptualization, Methodology, Validation, Supervision. **Timur Sh. Atabaev:** Conceptualization, Methodology, Validation, Resources, Writing – review & editing, Supervision.

#### Declaration of Competing Interest

The authors declare that they have no known competing financial

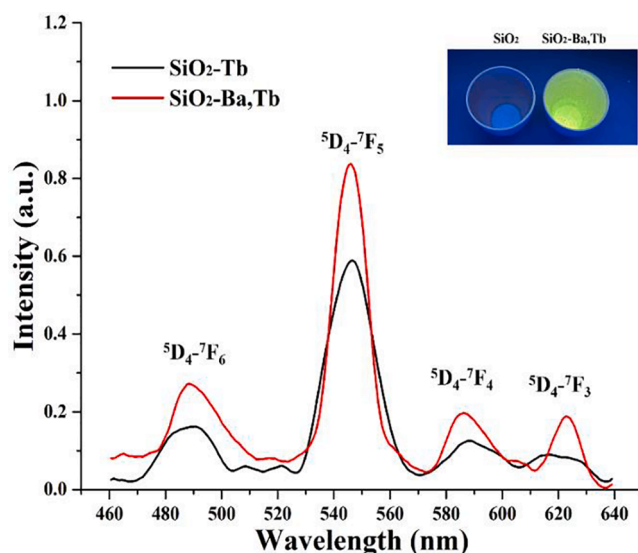


Fig. 4. PL emission spectra of SiO<sub>2</sub>-Tb and SiO<sub>2</sub>-Ba,Tb NPs. The inset is a digital image of bare SiO<sub>2</sub> (non-luminescent) and SiO<sub>2</sub>-Ba,Tb (luminescent) NPs under UV excitation ( $\lambda_{\text{exc}} = 254$  nm).

interests or personal relationships that could have appeared to influence the work reported in this paper.

#### Appendix A. Supplementary data

Supplementary data to this article can be found online at <https://doi.org/10.1016/j.matlet.2022.132500>.

#### References

- [1] Y. Yang, *Microchim. Acta* 181 (2014) 263–294.
- [2] Z. Yu, C. Eich, L.J. Cruz, *Front. Chem.* 8 (2020) 496.
- [3] Y. Zhong, H. Dai, *Nano Res.* 13 (2020) 1281–1294.
- [4] A.R. Mukhametshina, A.R. Mustafina, N.A. Davydov, et al., *Langmuir* 31 (2015) 611–619.
- [5] S.V. Fedorenko, A.R. Mustafina, A.R. Mukhametshina, et al., *Mater. Sci. Eng. C* 76 (2017) 551–558.
- [6] G.-L. Davies, J. O'Brien, Y.K. Gun'ko, *Sci Rep.* 7 (2017) 45862.
- [7] M. Tagaya, T. Ikoma, T. Yoshioka, S. Motozuka, F. Minami, J. Tanaka, *Mater. Lett.* 65 (2011) 2287–2290.
- [8] C. Lin, Y. Song, F. Gao, et al., *J. Sol-Gel Sci. Technol.* 69 (2014) 536–543.
- [9] A. Molkenova, Z. Oteulina, T.S. Atabaev, *Results Mater.* 11 (2021), 100209.
- [10] M.K. Mahata, T. Koppe, T. Mondal, et al., *Phys. Chem. Chem. Phys.* 17 (2015) 20741–20753.
- [11] D. González Mancebo, A.I. Becerro, A. Corral, et al., *ACS Omega* 4 (2019) 765–774.
- [12] T.S. Atabaev, Z. Piao, Y.-H. Hwang, H.-K. Kim, N.H. Hong, *J. Alloys Compd.* 572 (2013) 113–117.
- [13] B. Liu, M. Gu, X. Liu, et al., *Appl. Phys. Lett.* 94 (2009), 061906.
- [14] H. Li, Y. Zhang, R. Huang, et al., *Opt. Mater. Express* 11 (2021) 2599.
- [15] C. Schlumberger, M. Thommes, *Adv. Mater. Interfaces* 8 (2021) 2002181.
- [16] A.A. Ansari, J.P. Labis, *J. Mater. Chem.* 22 (2012) 16649–16656.
- [17] A.A. Ansari, J. Labis, A.S. Aldwayyan, M. Hezam, *Nanoscale Res. Lett.* 8 (2013) 163.
- [18] A.L. Fanai, U. Khan, S. Rai, *AIP Conf. Proc.* 2220 (2020), 080018.
- [19] T.S. Atabaev, H.H.T. Vu, Y.D. Kim, et al., *J. Phys. Chem. Solids* 73 (2012) 176–181.
- [20] A. Patra, P. Ghosh, P.S. Chowdhury, et al., *J. Phys. Chem. B* 109 (2005) 10142–10146.
- [21] Y. Liu, J. Wei, X. Yan, et al., *Chin. Chem. Lett.* 32 (2021) 861–865.